



## Behaviour of Full Scale Reinforced Concrete Beams Strengthened with Textile Reinforced Mortar (TRM)

Fawwad Masood<sup>1</sup>, Asad-ur-Rehman Khan<sup>2\*</sup>

<sup>1,2</sup> Department of Civil Engineering, NED University of Engineering &  
Technology, Pakistan

<sup>1</sup>fawwad@neduet.edu.pk, <sup>2\*</sup>asadkhan@neduet.edu.pk

Corresponding Author: Asad-ur-Rehman Khan

<https://doi.org/10.26782/jmcms.2019.06.00006>

### Abstract

*With increase in use of fibres for strengthening of Reinforced Concrete (RC) beams, Textile Reinforced Mortar (TRM) is becoming a popular choice among the researchers and scientists. While Carbon, glass and PBO fibers have shown encouraging results for structural strengthening, use of basalt fibres have not been much explored for strengthening other than masonry. Limited small-scale data exists for the use of basalt fibres in TRM strengthening but data for full scale beams is scarce. This paper presents an experimental study of six full scale RC beams tested with a varying shear span to depth ( $a/d$ ) ratio 3 through 6, where three beams served as control beams for various  $a/d$  ratios while the remaining three beams were strengthened with TRM using basalt fibres. TRM was provided at the tension face of the beams for strengthening in flexure along with U-shaped wraps. Results showed that TRM using basalt fibres is effective in improving the performance of RC beams in terms of serviceability, crack and deflection control, load carrying capacity, initial and post cracking stiffness, and ductility.*

**Keywords :** Reinforced concrete, Full scale beams, Strengthening, Textile Reinforced Mortar, Load-Deflection, Performance

### I. Introduction

The aging of structures and loss of strength due to damages result in reduction of load carrying capacity of existing buildings and infrastructure [XXIII]. Need of strength restoration or upgradation may arrive due to high traffic volumes in case of bridges and impact loading[XI], beside corrosion and increase in service loads[X]. The continuous introduction of more stringent building code requirements also plays its role in defining the need of strengthening of structures or their components[XXVII]. Strengthening of structures is an important issue as far green economy is concerned. Specifically, restoration and/or strengthening of reinforced concrete (RC) structures frequently require going through various strengthening techniques[XIII]. In the case of shear capacity, special attention is

needed since shear collapse is sudden and does not give sufficient warnings for pre-failure preventive measures.

The role of fibre reinforced composites has been an area of attention for researchers in recent decades for upgradation and strengthening of structures, particularly those made of Reinforced Concrete (RC). Fibre Reinforced Polymers (FRPs), have been frequently used in this regard both for research purposes [III],[XI],[XXII],[XXXI] and in strength upgradation of existing structures due to various reasons like upgradation of design codes, deterioration in structural members due to unforeseen loads, under design, change of usage modes etc. Despite of successful use of FRP for of strength upgradation, there are a few drawbacks associated with FRP which have been identified by researchers, which include high initial cost, reduced fire resistance, potentially harmful solvents for workers involved in the installation of FRPs, poor applicability of FRP on moist surface and at colder temperatures[XXIX]. Researchers have investigated usage of cementitious binding materials which may replace the epoxies used with FRPs and help overcome the above-mentioned problems. The interaction between fibre and matrix is replaced by orthogonally placed grids of fibre, held together by knitting the fibre roving. The spacing between the roving can be varied while manufacturing and will govern the mechanical properties of the textile grids and the dissemination of the cementitious mortar through the openings. The cementitious material should possess high workability along with adequate shear strength to restrain early de-bonding. The combination of these fibre grids and cementitious matrix is commonly termed as Textile Reinforced Mortar (TRM).

TRM has been explored with different names by various researchers, as mentioned by Triantafillou et. al. [XXIX] and its contribution has expressed encouraging results specially when used with carbon[XX],[XXVII], glass[X],[XXVII] and PBO [IV],[XII],[XVIII],[XXIV] fibres, with both in terms of load carrying capacity and also in terms of deflection and crack control[X],[XVII],[XXX]. However, Basalt fibres are mostly used for strengthening purpose for masonry construction and also for columns[IX],[XIX]. Effectiveness of the same is not much explored for full scale flexural members, although there has been an encouraging number of studies done on small and medium scale beams [VI], [XIII], [XVI], [XVIII], [XXI], [XXVI], [XXVIII],[XXXII]. The usage of Basalt fibres in Fibre-Reinforced concrete (FRC) has also shown better performance in terms of improvement in tensile and flexural properties of concrete and has shown encouraging bond behaviour between cementitious matrix and basalt fibres[V], [XV].

The existing research show that U-shaped wraps have been very effective in terms of strength [VI],[XXVI],[XXX],[XXXII]. Most of the existing studies also have focused on one to two shear span ratios, and thus not encompassing the flexural dominant region from shear span to depth ratios 3 through 6. This study explores the effectiveness of basalt fibres in conjunction with cementitious mortar for the strengthening and stiffness of flexural members using flexural strips along with U-wraps to compensate for additional shear that may arise due to increase in flexural capacity of due to application of TRM. Control and TRM strengthened beams were tested to failure under three-point bending.

## II. Experimental Program

### Control and Strengthened Reinforced Concrete Beams

Six full scale beams were selected for the purpose. Three beams were taken as control beams, one each for various  $a/d$  ratios (3, 4 and 6), while the rest of the three were strengthened using Textile Reinforced Mortar (TRM) having basalt fibre mesh, one each for the corresponding  $a/d$  ratios of 3, 4 and 6.

The clear span of the beams was 5485 mm (18') each, with a cross section of 300 mm  $\times$  458 mm (12"  $\times$  18"). Supports on each side were placed 230 mm away from the ends. Longitudinal reinforcement was taken as  $2 \times \rho_{\min}$  as per ACI 318-08 code [II] i.e.  $\rho = 0.67\%$ . All the beams were reinforced with four 16 mm dia. longitudinal bars at the bottom, and two 12 mm dia. bars at the top. Transverse shear reinforcement, 10 mm dia. bar, was provided at 200 mm (8") centre to centre in the shear span to ensure that beam fails in flexure for all shear span to depth ratios ( $a/d$ ) varying from 3 to 6. Concrete cover was 50 mm at top and bottom and 25 mm on the sides. Details of reinforced concrete beams used in the study are shown in Fig. 1, where "a" represents the varying shear spans as mentioned in Table 1.

TRM strips were applied at the bottom of the beams for strengthening in flexure along with the U-shaped wraps to prevent and premature debonding of the TRM strips and also to ensure that failure mode of the beams remains flexure. Length of the TRM strips in flexure was defined on the basis of assumption that flexure capacity can increase 100% after the application of TRM and TRM strips were provided up to the point where the moment capacity in enhanced bending moment diagram reaches actual moment capacity of the control beams. U-wraps were applied from support to the point of load application (shear span) and then extended to the distance equal to the shear span on the other side, making the total length of the TRM U-wrap twice of the shear span. If the length of TRM U-wrap exceeded the length of flexural TRM strip, the same length of flexural strip as that of U-wrap was provided, which only happened in the case of shear span to depth ratio 6. The details of TRM lengths for flexure and shear are given in Table 1 and shown in Fig. 2. Nomenclature of control and TRM strengthened beams is given in Table 2.

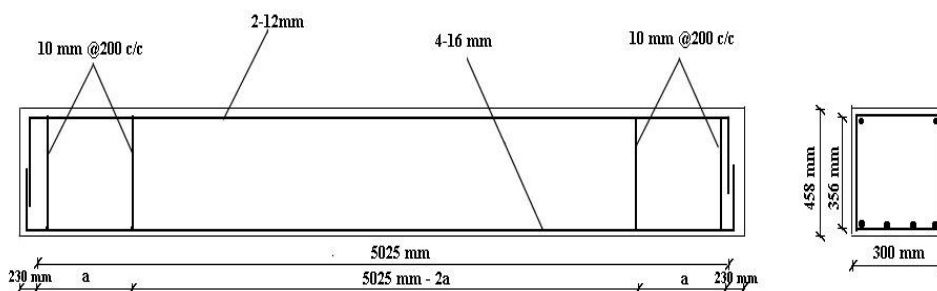


Fig. 1 Reinforcement details and dimensions of all the beams

Table 1. Details of distance variation according to a/d ratios

a/d ratio	Distance (a) from left support	Length (2a) of TRM U-Wrap	Length of TRM Flexural strip (2a+e)
3	1218	2436	3352
4	1625	3250	3556
6	2435	4870	4870

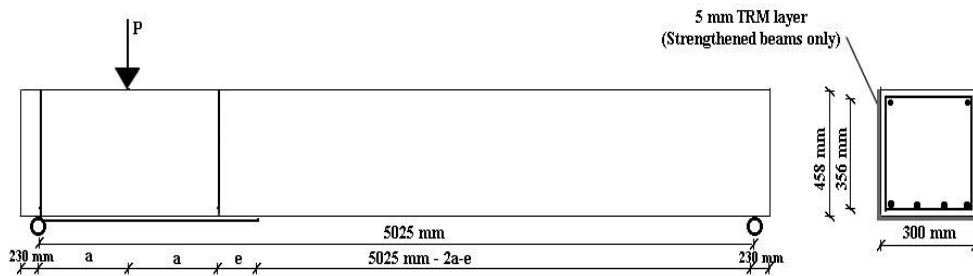


Fig. 2Details of TRM strip length and U-wraps

Table 2. Nomenclature of Control and Strengthened Beams

S. No	Beam ID	Beam Description
1	CT3	Control beam with shear span a = 1218 mm (a/d = 3.0)
2	CT4	Control beam with shear span a = 1625 mm (a/d = 4.0)
3	CT6	Control beam with shear span a = 2435 mm (a/d = 6.0)
4	TRM3	TRM Strengthened beam with shear span a = 1218 mm (a/d = 3.0)
5	TRM4	TRM Strengthened beam with shear span a = 1625 mm (a/d = 4.0)
6	TRM6	TRM Strengthened beam with shear span a = 2435 mm (a/d = 6.0)

### Material Properties

The concrete used for the beams had a 28 days compressive strength of 20.68 MPa (3 ksi) while the steel used for longitudinal reinforcement was of yield strength 500 MPa (72 ksi) and shear reinforcement was of yield strength 413.68 MPa (60 ksi).

Compressive strength of mortar, Tyfo C-Matrix provided by the manufacturer, to be used as matrix binder, was found to be 26.2 MPa (3.8 psi) for 28 days cured specimens. The gross tensile strength of the TRM system with embedded fibres and adhesion to base strength/bond strength, as provided by the manufacturer, were 7 Mpa (1.11 ksi) for 28 days cured specimens and 1.5 Mpa (0.218 ksi) respectively. Table 3 shows the gross properties of TRM matrix as provided by the manufacturer.

Table 3. Tyfo RM System Gross Properties (EP-B with C-Matrix)

Property	Typical Test Value	Design Value
Ultimate tensile strength, MPa	6.00	5.10
Elongation at ultimate	1.62%	1.62%
Tensile Modulus, GPa	0.37	0.31
Layer Thickness, mm	5	5

### Application of TRM

Surfaces of the beams were first prepared as per the recommendations of the manufacturer. Loose dust particles and sharp edges or other irregularities were smoothed using grinder. The beam edges were rounded to a radius of 2 cm. Before application of TRM, humidification of the surface was performed so that the water mixed within the matrix may not be lost in making the concrete surface moist. 200 ml of water per kg of Tyfo C-Matrix was taken which was the upper bound limit as recommended by the manufacturer to acquire required workability and consistency and was mixed at a mixing rate of 400-600 rpm for 5-10 minutes.

A 2 mm layer was applied on the already prepared surface of concrete with the help of trowel. The layer of Tyfo EP-B fabric, appropriately cut to the required length, was then applied by hand pressure carefully laying out onto the mortar surface and smoothed out to make sure that the fibres are straight and well impregnated with the mortar. Another layer of Tyfo C-matrix was applied on the fabric to fully cover the fabric, resulting in a net overall thickness of 5 mm. The surface was smoothed using trowel. Strengthened beams were further cured for 28 days after TRM application. Fig. 3 shows the process of TRM application on the strengthened beams. It is to be noted that RC beams to be strengthened were pre-cracked before the application of TRM.

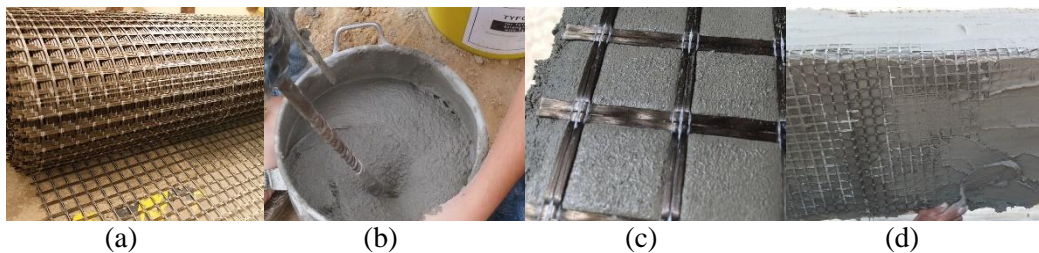


Fig. 3 Process of TRM Application

### III. Experimental Setup

All the control and strengthened beams were tested under three-point bending. The location of application of load varied according to the shear span to depth ratios under consideration and is already given in Table 1. The support to support distance for all the beams was 5485mm. LVDTs were placed under the load and at mirrored location from the far end to observe deformation. Surface and embedded strain gauges were also installed on compression face, flexural

reinforcement level, extreme TRM fibregand location of expected shear crack to monitor strains. Load was applied at a distance  $a$ (Fig.2) at the rate of 0.01 mm/sec. Testing arrangement is shown in Fig. 4.

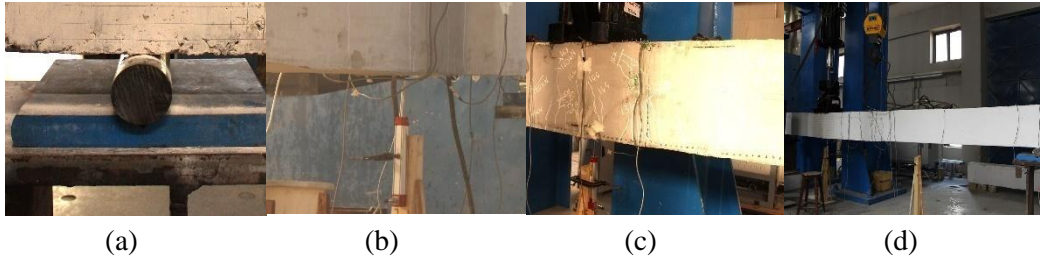


Fig. 4 Testing arrangement of control and TRM strengthened beams

#### IV. Results and Discussion

This section presents the results in terms of load carrying capacities, crack patterns, first cracking loads, load-deflection curves, initial stiffness, post-cracking stiffness, performance factor and ductility of control and TRM strengthened beams for each  $a/d$  ratio in detail in the subsections to follow.

##### Load Carrying Capacities

Table 4 presents the summary of maximum loads as taken by the control and strengthened beams, along with the percentage gain in the failure load for strengthened beams and their respective failure modes.

TRM3 showed a relatively smaller gain in load carrying capacity of around 3%. Beams TRM4 and TRM6 however, showed decent increment in load carrying capacity, i.e. 19 and 30% respectively, showing that Basalt fibre TRM is more effective for strengthening as shear span to depth ratio is increased in flexural critical region.

Table 4. Summary of failure loads as taken by the beams and the failure modes.

S No.	$a/d$ ratio	Control Beam Load	Control Beam Mode	Strengthened Beam Load	Strengthened Beam Mode	Percentage Increase
1	3	188	Flexure	192.5	Flexure	3%
2	4	143	Flexure	170	Flexure	19%
3	6	107	Flexure	139	Flexure	30%

##### First Cracking Loads and Crack Pattern

Table 5 shows the observed values of first cracking load during the experiment for control and TRM Strengthened Beams and the percentage increase after application of TRM.



Table 5. Values of Cracking loads for the beams

a/d	Flexural Cracks			Shear Cracks		
	Control Beams	TRM Beams	% Increase	Control Beams	TRM Beams	% Increase
3	30 kN	55 kN	83	114 kN	123 kN	8
4	26 kN	48 kN	85	-	-	-
6	10 kN	20 kN	100	-	-	-

All the control beams had the first flexural crack at the point of maximum moment, i.e. under the point load. As the loading continued more cracks appeared in the vicinity of the major flexural crack depicting the classical flexural failure. For TRM strengthened beams, major flexural crack appeared under the load which was followed by closely spaced and well distributed hairline cracks. Each TRM strengthened beam showed classical flexural failure with better distribution of cracks.

It can be observed that TRM wraps applied for flexure strengthening contributed significantly in increasing the cracking load for strengthened beams. Impact of strengthening on first flexural cracking load of beams for a/d ratios 3 to 6 varies from 83-100%, reflecting the effectiveness of TRM in flexural crack control for flexural critical regions. Since the beams were strengthened primarily in flexure, no shear cracks were observed in control and strengthened beams for a/d ratios of 4 and 6. Few shear cracks, however, were observed for a/d ratio of 3. It can be seen that application of TRM was also effective in delaying shear cracking.

Crack patterns and spacing for all control and TRM strengthened beams at failure are shown in Fig. 5 and discussed in following sections.

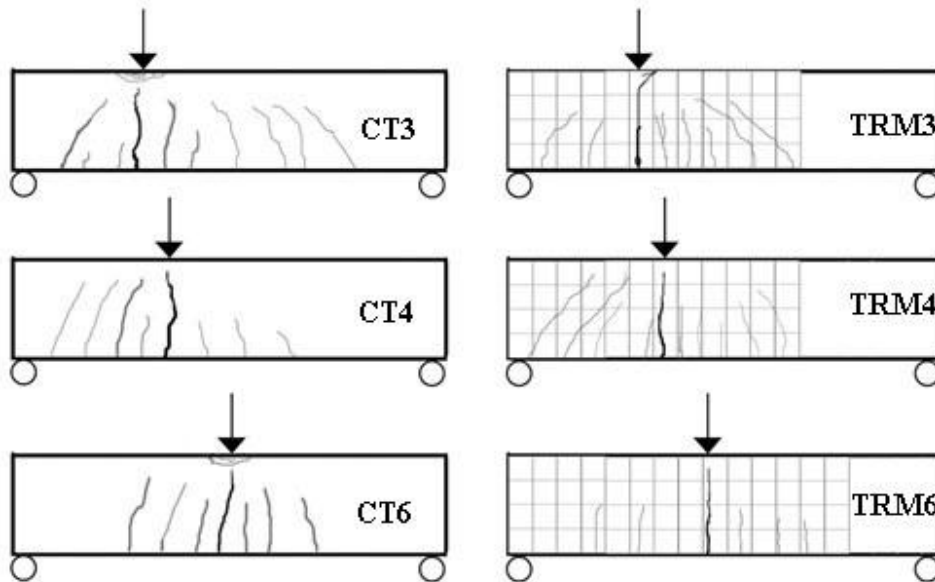


Fig. 2 Crack patterns and crack spacing of control and strengthened beams at failure

### **a/d ratio 3**

For beam CT3, first flexural crack appeared at the point of maximum moment, followed by hairline flexural cracks widely spaced. As the load was increased, a hairline shear crack appeared which was arrested by the reinforcement present and thus the beam kept taking load until it reached flexural failure. The flexural cracks grew wider as the loads progressed. The beam reached failure in flexural mode with yielding of reinforcement followed by the crushing of concrete at the top. The width of the governing flexural crack was observed to 2 mm at the failure. A wider flexural crack was observed next to the governing crack. The other flexural cracks are widely spaced and thus have consider widths.

For beam TRM3, the governing flexural crack is 1.5 mm at the time of crushing of concrete, which is considerably narrower as it progresses towards the compression zone, in comparison with the corresponding control beam. The other cracks in the flexural zone are visibly narrow in width and are closely and uniformly spaced.

### **a/d ratio 4**

In case of beam CT4 the governing flexural crack at the time of crushing of concrete was observed to be 2 mm in thickness. The nearby cracks in the flexural zone have considerable width. The flexural cracks are widely spaced. The major flexural crack had significant width while moving towards the compression face.

Beam TRM4 failed with crushing of concrete at the top, with the width of major flexural crack being 1.5 mm. The rest of the flexural cracks are closely spaced and have almost hairline appearance, well distributed over the flexural zone.

### **a/d ratio 6**

BeamCT6 failed in flexure with visible crushing at the compression concrete face. The major flexural crack had a width of 2 mm at the time of failure. The surrounding flexural cracks were widely spaced and had considerable widths ranging around 1 to 1.5 mm.

BeamTRM6, which failed in flexure, had the width of major flexural crack 1.5 mm. The crack grew narrower as it moved towards the neutral axis and then compression zone. The other cracks in flexural zone are closely spaced and almost showed hairline appearance.

The comparison of cracking behaviour of control beams with the corresponding TRM strengthened beams show an overall improvement in terms of cracking behaviour. In case of strengthened beams, the crack widths of the governing cracks were noticeably reduced, while the cracks in the nearby flexural zone were equally spaced and well spread with lesser thickness as compared to their respective control beam.

### **Load-Deflection Curves**

The following section discusses the load-deflection curves for control and strengthened beams for all shear span to depth ratios.



### **a/d ratio 3**

Load-deflection curves of beams CT3 and TRM3 are presented in Fig. 6. Both the beams, CT3 and TRM3, showed hairline shear crack which was arrested by the shear reinforcement and also TRM layer in case of TRM3 beam. The TRM beam showed more post cracking stiffness as compared to the control beam. The control beam yielded at a load of 177kN and a deflection of 25.03 mm While the TRM3 beam yielded at a load of 178kN and a deflection of 20.41 mm. The ultimate load taken by the control beam was 188kN and a deflection of 35.48 mm while for TRM beam it was 192kN with a deflection of 27.45 mm.

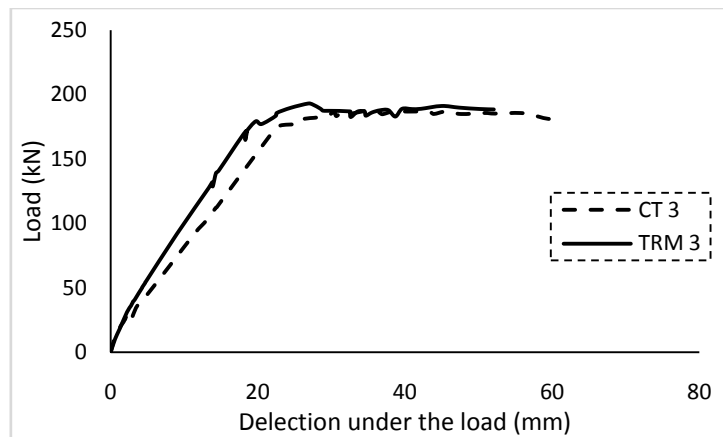


Fig. 3 Load-Deflection curves of control and strengthened beams for a/d ratio 3

### **a/d ratio 4**

Fig. 7 represents the load-deflection curves of beams CT4 and TRM4. Beams CT4 and TRM4 showed shear crack which was arrested by the shear reinforcement (and TRM layer in case of TRM4 beam). The TRM strengthened beam again showed more post cracking stiffness as compared to the control beam. The control beam yielded at a load of 138kN and a deflection of 28.34 mm While the TRM4 beam yielded at a load of 158kN and a deflection of 27.29 mm. The ultimate load taken by the control beam was 143kN and a deflection of 45.56 mm while for TRM4 beam it was 169 kN with a deflection of 51.48 mm.

### **a/d ratio 6**

Load-deflection curves of beams CT6 and TRM6 are shown in Fig. 8. Both the beams CT6 and TRM6 showed flexural cracking in maximum moment region which widened as the load application progressed. The control beam yielded at a load of 102kN and with a deflection of 27.38mm. While the TRM6 beam yielded at a load of 126kN and a deflection of 29.31 mm. The ultimate load taken by the control beam was 107 kN and a deflection for three-point bending of 54.91 mm while for TRM beam it was 139 kN with a deflection of 50.59 mm. Fig. 8 represents the load-deflection curves of beams CT6 and TRM6.

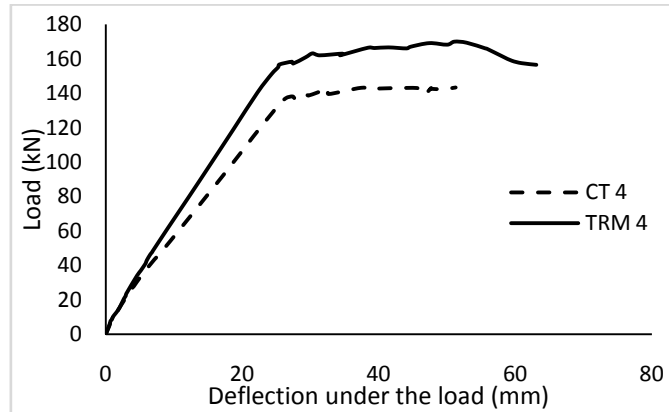


Fig. 4 Load-Deflection curve for a/d ratio 4 for control and strengthened beams

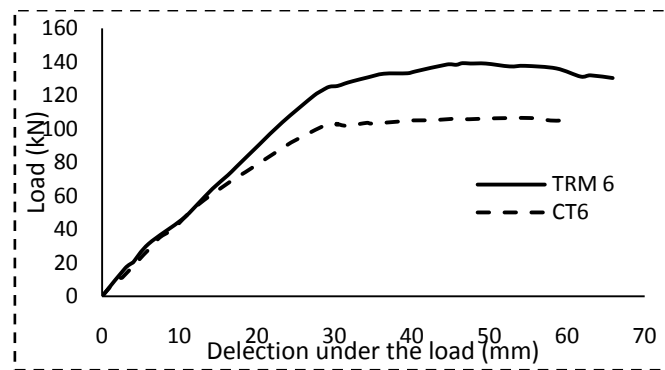


Fig. 5 Load-Deflection curve for a/d ratio 6 for control and strengthened beams

It can be noted from the preceding discussion and Figs. 6 – 8 that application of TRM influenced the post-cracking behavior of the strengthened beams resulting in the increased stiffness and better performance as discussed in following sections.

### Initial and Post-cracking Stiffness

The initial or pre-cracking stiffness is compared to observe if there is any influence of TRM strengthening on the pre-cracking stiffness, which may be observed in some other methods of strengthening like FRP wraps and/or strips. For all the beams (Fig. 6 to 8), the stiffness does not differ much in either control or strengthened beams, since TRM is not playing its role before the appearance of the cracks. Study of post cracking stiffness shows that TRM has played a visible part in increasing the beam stiffness of strengthened beam in post cracking region, thus playing a significant role in terms of serviceability.

Beam TRM3 shows visible difference (Fig. 6) in stiffness right from the point of cracking and the same behaviour goes throughout until failure load is achieved. TRM4 also shows improvement in stiffness in a manner similar to that shown by the specimens tested for a/d ratio 3. TRM6 beam when compared to CT6 shows a significant increment in stiffness as the loading increases.

Table 6 presents the values of slope of load versus deformation curve in pre and post cracking regions and the drop of post cracking stiffness for all control and strengthened beams.

Table 6. Slope of Load-deflection curve in post cracking region.

Beam	Slope in pre-cracking region	Slope in post-cracking region	Loss of Stiffness after cracking (%)
CT3	11.7	7.24	38
TRM3	11.45	8.31	27
CT4	7.02	4.92	30
TRM4	7.03	5.88	16
CT6	5.21	3.22	38
TRM6	5.10	4.25	16

The values of gradient of load-deflection curve in pre-cracking region are consistent for control and TRM beams for a given  $a/d$  ratio. However, the gradient in post-cracking region shows a drop for all  $a/d$  ratios. The drop in post-cracking gradient of load-deflection curves for control beams is higher as compared to TRM strengthened beams, which shows the effectiveness of TRM in serviceability. By comparing the three  $a/d$  ratios used, the effectiveness of TRM in terms of loss of stiffness in post-cracking region and thus in serviceability is significantly higher in case of  $a/d$  ratios 4 and 6 as compared to  $a/d$  ratio of 3, which means  $a/d$  is more effective in increasing the stiffness of flexure controlled beams.

### **Relative Ductility**

The relative ductility is calculated by taking the difference of deformations at ultimate and yield loads. It is important to note that the value of deformation at ultimate was taken at the farthest point with 1% variation from the highest load achieved for a given set of specimens. Table 7 represents the values of deformations at yield and ultimate and the difference of values of deformation between yield and ultimate.

The values of deformation at yield for each control and the corresponding TRM strengthened beam are almost comparable. However, significant increase in deformation at ultimate is observed, except for  $a/d$  ratio 6, which resulted in sufficient warning before failure. The effectiveness of improvement in ductility enhancement does not appear to be significant in the case of TRM6 because the control beam CT 6 has already shown significant increase in deformation at ultimate.

Table 7. Relative Ductility for control and strengthened beams

Beam	Deformation at yield (mm)	Deformation at Ultimate (mm)	Difference of Deformation (mm)
CT3	22.09	35.7	13.61
TRM3	20.5	52.1	31.6
CT4	26.35	45.76	19.41
TRM4	25.25	53.4	28.15
CT6	30.38	59.16	28.77
TRM6	29.31	58.59	29.28

### Performance Factor Based on Load and Deformation

To measure the performance of TRM strengthening system, a reliable methodology may be considering strength and deformability simultaneously. A viable strengthening solution should have an optimized combination of both while being designed [XXV]. For comparison purposes, the load and deformation may be calculated by taking the corresponding values at limit and ultimate states respectively for control and corresponding strengthened beam. It has been reported in literature to consider a compressive strain of 0.001 in concrete as the starting point of nonlinear structural performance [VII].

Deformability factor (DF) and Strength factor (SF) can then be defined as follows (Spadea et. al. [XXV]):

$$DF = \frac{\text{Deflection at ultimate limit state}}{\text{Deflection at } \epsilon_c = 0.001} \quad (1)$$

$$SF = \frac{\text{Load at ultimate limit state}}{\text{Load at } \epsilon_c = 0.001} \quad (2)$$

The overall structural performance of the strengthened composite beam can thus be evaluated by a global factor defined as Performance factor (PF), integrating strength and deformability, both weighted equally (Spadea et. al. [XXV]). This Performance Factor is defined as:

$$PF = DF \times SF \quad (3)$$

Table 8 summarizes the resulting deformability, strength and corresponding performance factors for the control and TRM strengthened beams. The values of DF for beams with a/d ratios 3 through 4 show notable improvement, while for a/d ratio 6 there is no significant effect on deformation factor in beam TRM6 in comparison with CT6. While for load factor SF, all the beams from a/d ratio 3 to 6 showed improvement, except for beam CT3 for which the factor remained almost the same. The results indicate that use of TRM has overall improved the performance of the RC beams both in terms of deformation and loads.

Table 8. Performance factors for control and TRM strengthened beams

Beam	DF	SF	PF	Performance Enhancement (%)
CT3	13.90	6.25	86.88	
TRM3	23.47	6.28	147.58	70
CT4	12.37	5.50	68.10	
TRM4	15.55	6.45	93.87	39
CT6	28.33	9.75	276.36	
TRM6	28.02	12.47	349.60	26.5

## V. Analytical Study

The subsections below discuss various approaches used for the calculation as given in the codes for FRP and TRM when used for strengthening purposes. The purpose of using the models below is to predict the ultimate shear resistance of the beams subjected to testing and compare the results with those obtained through the codes. For the codes and modules originally meant for FRP, the formulation is adapted according to the characteristics for TRM.

### Fib-Bulletin 14 model

The Fib-Bulletin [XIV] suggests eq (4) for the contribution of FRP fibres, which almost follows the same approach as followed by the other codes under discussion except for minor changes. The contribution of steel is taken in the same way, by taking the product of area of steel  $A_s$  and yield strength of steel  $f_{yd}$ . For the centroid of equivalent stress is calculated, however in a slightly different manner, where the factor  $\delta_G$  is taken as 0.4. The contribution of fibres is calculated by taking the area of fibres applied and the stress is obtained by taking the product of modulus of the fibre reinforcement  $E_f$  applied (which is taken as 0.67 GPa) and the strain  $\epsilon_f$  (1.62%) in the fibres. The value of neutral axis  $x$  is obtained by using compression versus tensile force equilibrium.

$$M_{Rd} = A_{s1}f_{yd}(d - \delta_G x) + A_f E_f \epsilon_f (h - \delta_G x) \quad (4)$$

Using the fib-bulletin 14 equation the moment capacity obtained for the control beam was found to be 130 kN-m, while for TRM strengthened beam the moment capacity of 132 kN-m, showing merely 1.73% increase of moment capacity of strengthened beam.

### ISIS Module

The ISIS module [VIII] uses the same basic approach to calculate the flexural capacity of RC beams with slight changes in capacity reduction factors and calculation of neutral axis. The ISIS module uses equivalent stress block for calculation of moment arm as used in ACI 318R-14 [II]. The force contribution by steel and fibres however, follow the same approach as used in fib-bulletin 14. The value of  $\epsilon_{frp}$  is calculated through strain compatibility and is found to be 0.89%,

which is less than the failure strain of TRM fibre which means that while the steel reinforcement yields while the TRM does not reach its failure strain. The ISIS module uses a different approach if the failure strain of fibres is reached. The equation given in ISIS module is as follows.

$$M_r = \varphi_s f_y A_s (d - a/2) + \varphi_{frp} A_{frp} E_{frp} \varepsilon_{frp} (h - a/2) \quad (5)$$

The capacity reduction factors  $\varphi_s$  and  $\varphi_{frp}$  were not considered to give a fair estimate of the actual moment capacity. The ISIS module estimated the moment capacity of control beam as 144 kN-m while for strengthened beam it gave a moment capacity of 149 kN-m, with a capacity increase of 3.55% making ISIS module less conservative in comparison with fib-bulletin 14 both in terms of capacity prediction and effectiveness of TRM.

### ACI 549.4R-13 Model

The approach followed by ACI 549.4R-13 [I] and ISIS module is almost the same. The depth of neutral axis and the moment arm follows the same procedure. However, the constants used to calculate the value of  $a$  from the neutral axis differs slightly, although the values obtained through either method are almost the same. The value of  $\varepsilon_{frp}$  is taken as 1.62% as provided by the vendor for comparison with actual results, ignoring the limit of 0.004 as mentioned by ACI 549.4R-13. The values of  $\varphi_s$  and  $\varphi_{frp}$  are not considered to compare with the actual results.

$$M_r = \varphi_s f_y A_s (d - a/2) + \varphi_{frp} A_{frp} E_{frp} \varepsilon_{frp} (h - a/2) \quad (6)$$

The ACI 549.4R-13 estimated the moment capacity of control beam as 148 kN-m while for strengthened beam it gave a moment capacity of 152 kN-m, with an increase of 2.48% moment capacity. The ACI 549.4R-13 gives the least conservative values for moment capacity while lesser increment in terms of capacity increase for strengthened beam. The difference in the values from ISIS modules and ACI 549.4R-13 is due to different values of strains, otherwise both equations would give almost the same values if the values of capacity reduction factors are not considered. Table 9 shows the experimental moment capacities as observed for each a/d ratio.

**Table 9.** Comparison of experimental ultimate moment capacities for control and TRM strengthened beams with various codes

a/d ratio	Experimental		ISIS Module		ACI 549.4R-13		Fib-Bulletin 14	
	Control (kN-m)	TRM (kN-m)	Control (kN-m)	TRM (kN-m)	Control (kN-m)	TRM (kN-m)	Control (kN-m)	TRM (kN-m)
3	178	183						
4	164	194	144	149	148	152	130	132
6	144	188						

For control beams, an average moment capacity of 162kN-m was observed with not much significant variation across the given a/d ratios, which is more than calculated



by any of the three design codes discussed above. For strengthened beams, the average moment capacity was found to be 188kN-m, showing a consistent impact of TRM strengthening on moment capacity of around 16% which is significant.

It may be noted that all the three codes discussed above predict very conservative effect of strengthening with a capacity gain ranging from 2 to 3.5%, while experimental results show a gain of around 16% as mentioned above.

## **VI. Conclusions**

The following inferences can be made from the above presented study:

- Application of TRM delayed the initial cracking, thereby increasing the initial cracking loads for both shear and flexure cracks. The percentage increase in flexural cracking loads increases significantly for a/d ratio 3,4 and 6 i.e. 83%, 85% and 100 % respectively. For shear cracking, the percentage increase in load was 8% for shear span to depth ratio 3, while no shear cracks appeared for a/d ratios 4 and 6 for both control and strengthened specimens.
- Application of TRM increased the ultimate loads with better results for a/d ratios 4 and 6 as compared a/d ratio 3, making it more effective for flexure critical beams as the shear span to depth ratio is increased.
- No significant change was observed in initial stiffness of control and strengthened beam specimens. Sizeable improvement in post-cracking stiffness in TRM strengthened beams was noted showing the effectiveness of basalt fibre TRM for flexural members.
- An improved relative ductility of the flexural members was observed for TRM strengthened beams, with higher deformations at ultimate loads. However, its influence differs with respect to shear span to depth ratios. The influence of TRM using Basalt fibres was found very effective for a/d ratio 3 and 4. But for a/d ratio 6 the beam TRM6 showed slight improvement in terms of relative ductility. This may be because the beams with a/d ratio 6 depict inherently significant ductile behaviour.
- Enhanced performance of TRM strengthened beams as compared to the control beams was predicted by performance factor as proposed by Sapde et al. [XXV] which takes into account deformation and strength together at ultimate and service loads.
- The theoretical flexural capacities as given by ISIS module, fib-bulletin 14 and ACI 594.5R-13 were found to be conservative for control and TRM strengthened beams. The prediction is more conservative in case of strengthened beams, with ISIS module and ACI 594.5R-13 predicting loads nearer to those observed in experiments. If the capacity reduction factors as suggested by each code are applied, then ACI 594.5R-13 tends to give the least conservative values.
- Overall, use of basalt fibre based Textile Reinforced Mortar played an effective role in improving the performance of the TRM strengthened beams.

## **VII. Acknowledgements**

The authors are grateful to the Department of Civil Engineering, NED University of Engineering and Technology and the aforementioned university itself, in the quest of this work. The authors also thankfully acknowledge Fyfe Co., LLC of Aegion Corporation, for providing the Textile Reinforced Mortar product Tyfo® C-Matrix for research purpose.

## **References**

- I. ACI. "Guide to design and construction of externally bonded fabric-reinforced cementitious matrix (FRCM) systems for repair and strengthening concrete and masonry structures",2013
- II. ACI Committee %J American Concrete Institute, F. H., MI. (2014). 318, "Building Code Requirements for Structural Concrete (ACI 318–14) and Commentary (ACI 318R–14). 519",2014
- III. Al-Salloum, Y. A., Siddiqui, N. A., Elsanadedy, H. M., Abadel, A. A., & Aqel, "Textile-reinforced mortar versus FRP as strengthening material for seismically deficient RC beam-column joints", *Journal of Composites for Construction* 15(6), 920-933, 2011
- IV. Aljazaeri, Z. R., Janke, M. A., & Myers, "A novel and effective anchorage system for enhancing the flexural capacity of RC beams strengthened with FRCM composites",*Composite Structures*, 2018
- V. Ayub, T., Khan, S. U., & Memon, F. Ahmed, (2014). "Mechanical characteristics of hardened concrete with different mineral admixtures: a review", *The Scientific World Journal*, 2014.
- VI. Azam, R., & Soudki, "FRCM strengthening of shear-critical RC beams",*Journal of Composites for Construction*, 18(5), 04014012, 2014
- VII. Bencardino, F., Spadea, G., Swamy, "The problem of shear in RC beams strengthened with CFRP laminates", *Construcion Building Materials*, 21(11), 1997-2006, 2007
- VIII. Bisby, L., & Williams, B. J., "An introduction to FRP strengthening of concrete structures". 4, 1-39, *ISIS Educational Module*, 2014
- IX. Bournas, D. A., Lontou, P. V., Papanicolaou, C. G., T. Triantafillou, "Textile-reinforced mortar (TRM) versus FRP confinement in reinforced concrete columns", *ACI Structural Journal* 104(6), 740-748, 2007
- X. Brückner, A., Ortlepp, R., Curbach, "Textile reinforced concrete for strengthening in bending and shear", *Materials & Structures* 39(8), 741-748, 2006

- XI. Carloni, C., Subramaniam, K. V., Savoia, M., & Mazzotti, "Experimental determination of FRP–concrete cohesive interface properties under fatigue loading". 94(4), Composite Structures, 1288-1296, 2012
- XII. D’Antino, T., Carloni, C., Sneed, L., & Pellegrino, "Matrix–fiber bond behavior in PBO FRCM composites: A fracture mechanics approach", Engineering Fracture Mechanics, 117, 94-111, 2014
- XIII. Escrig, C., Gil, L., Bernat-Maso, E., Puigvert, "Experimental and analytical study of reinforced concrete beams shear strengthened with different types of textile-reinforced mortar", Construction and Building Materials, 83, 248-260, 2015
- XIV. Fib bulletin:"Externally Bonded FRP Reinforcement for RC Structures". (14), 51-58., 2001
- XV. Jiang, C., Fan, K., Wu, F., Chen, "Experimental study on the mechanical properties and microstructure of chopped basalt fibre reinforced concrete", Materials & Design 58, 187-193, 2014
- XVI. Khan, A., F. Masood, "Strengthening of Reinforced Concrete Beams With Textile Reinforced Mortar (TRM) in Flexure", 8th International Civil Engineering Congress (ICEC-2016), Karachi, Pakistan, 2016
- XVII. Khan, A., F. Masood, "Strengthening of shear deficient reinforced concrete beams with textile reinforced mortar (TRM)".8th international conference on fibre-reinforced (FRP) composites in civil engineering, Hong Kong, China, 2016
- XVIII. Loreto, G., Babaeidarabad, S., Leardini, L., & Nanni, "RC beams shear-strengthened with fabric-reinforced-cementitious-matrix (FRCM) composite", International Journal of Advanced Structural Engineering7(4), 341-352, 2015
- XIX. Ma, G., G. Li, "Experimental study of the seismic behavior of predamaged reinforced-concrete columns retrofitted with basalt fiber–reinforced polymer", Journal of Composites for Construction, 19(6), 04015016, 2015
- XX. Ombres, L., Mancuso, N., Mazzuca, S., & Verre, "Bond between Carbon Fabric-Reinforced Cementitious Matrix and Masonry Substrate", Journal of Materials in Civil Engineering, 31(1), 04018356, 2018
- XXI. Ombres, Luciano, "Structural performances of reinforced concrete beams strengthened in shear with a cement based fiber composite material", Composite Structures, 122, 316-329, 2015
- XXII. Razaqpur, A. G., Shedid, M., & Isgor, Burkan, "Shear strength of fiber-reinforced polymer reinforced concrete beams subject to unsymmetric loading", Journal of Composites for Construction, 15(4), 500-512, 2010
- XXIII. Rostam, S., Bakker, R., Beeby, A., van Nieuwenburg, D., Schiessl, P., L. Sentler, "Durable Concrete Structures-CEB Design Guide", Bulletin d’Information (182), 1992

- XXIV. Sneed, L., D'Antino, T., Carloni, C., Pellegrino, C., "A comparison of the bond behavior of PBO-FRCM composites determined by double-lap and single-lap shear tests", *Cement and Concrete Composites*, 64, 37-48, 2015
- XXV. Spadea, G., Bencardino, F., Swamy, R. J. M., "Optimizing the performance characteristics of beams strengthened with bonded CFRP laminates", *Materials and Structures*, 33(2), 119-126, 2000
- XXVI. Tetta, Z. C., Koutas, L. N., & Bournas, D., "Textile-reinforced mortar (TRM) versus fiber-reinforced polymers (FRP) in shear strengthening of concrete beams", *Composites Part B: Engineering*, 77, 338-348, 2015
- XXVII. Tetta, Z. C., Koutas, L. N., & Bournas, D., "Shear strengthening of full-scale RC T-beams using textile-reinforced mortar and textile-based anchors", *Composites Part B: Engineering*, 95, 225-239, 2016
- XXVIII. Trapko, T., Urbańska, D., & Kamiński, M., "Shear strengthening of reinforced concrete beams with PBO-FRCM composites", *Composites Part B: Engineering*, 80, 63-72, 2015
- XXIX. Triantafillou, T. C., Papanicolaou, C. G., Zissimopoulos, P., & Laourdekis, T., "Concrete confinement with textile-reinforced mortar jackets", *ACI Materials Journal*, 103(1), 28, 2006
- XXX. Triantafillou, T. C., Papanicolaou, C., "Shear strengthening of reinforced concrete members with textile reinforced mortar (TRM) jackets", *Materials & Structures*, 39(1), 93-103, 2016
- XXXI. Triantafillou, T., "Shear strengthening of reinforced concrete beams using epoxy-bonded FRP composites", *ACI Structural Journal*, 95, 107-115, 1998
- XXXII. Tzoura, E., Triantafillou, T. J. M., & Structures. (2016). "Shear strengthening of reinforced concrete T-beams under cyclic loading with TRM or FRP jackets", *Materials & Structures*, 49(1-2), 17-28, 2016